Trpc6 knockout protects against renal fibrosis by restraining the CN-NFAT2 signaling pathway in T2DM mice

RAN SUN[1*], MIN HAN[1*], YAN LIU[1*], YONG SU[2], QIFENG SHI[1], LEI HUANG[1], LIANGLIANG KONG[1], WEIZU LI[1] and WEIPING LI[1]

[1]Department of Pharmacology, Grade III Laboratory of National Administration of Traditional Chinese Medicine, School of Basic Medical Sciences, Anhui Medical University; [2]Department of Pharmacy, The First Affiliated Hospital of Anhui Medical University, Hefei, Anhui 230032, P.R. China

Received August 24, 2023; Accepted October 30, 2023

DOI: 10.3892/mmr.2023.13136

Abstract. Diabetic kidney disease (DKD), one of the common complications of type-2 diabetes mellitus (T2DM), has become the principal cause of end-stage kidney disease. Transient receptor potential channel 6 (TRPC6), one of non-selective cation channels with significant calcium-permeability, is associated with renal fibrosis. However, the mechanism of TRPC6 in T2DM-induced renal fibrosis is still not entirely understood. The present study explored the potential mechanism of *Trpc6* knockout in T2DM-induced renal fibrosis in *Trpc6*$^{-/-}$ mice. The results showed that *Trpc6* knockout inhibited the loss of body weight and the increase of fasting blood glucose (FBG) and significantly improved renal dysfunction and glomerular fibrosis in T2DM mice. The present study also indicated that *Trpc6* knockout significantly lowered the expression of phosphorylated (p-)SMAD2/3, TGF-β, calcineurin (CN), nuclear factor of activated T-cell (NFAT)2 and Nod-like receptor (NLR) 3 inflammasome-associated proteins. Calcium imaging results revealed that *Trpc6* knockdown could decrease the levels of $[Ca^{2+}]_i$ and inhibited calcium homeostasis imbalance. Moreover, it was found that knockout of *Trpc6* had no significant influence on lipid disposition and reactive oxygen species generation in the kidney cortex. The present study suggested that knockout of *Trpc6* may alleviate glomerular fibrosis and delay DKD progression by reducing $[Ca^{2+}]_i$ overload and inhibiting the CN-NFAT2 pathway in T2DM mice.

Correspondence to: Professor Weizu Li or Professor Weiping Li, Department of Pharmacology, Grade III Laboratory of National Administration of Traditional Chinese Medicine, School of Basic Medical Sciences, Anhui Medical University, 81 Meishan Road, Hefei, Anhui 230032, P.R. China
E-mail: liweizu@126.com
E-mail: lwp19@126.com

*Contributed equally

Key words: type-2 diabetes mellitus, renal fibrosis, transient receptor potential channel 6, nuclear factor of activated T-cell 2, Nod-like receptor protein 3 inflammasome

Introduction

Type-2 diabetes mellitus (T2DM) is one of the most common metabolic diseases, characterized by chronic hyperlipidemia and hyperglycemia. With the incidence of T2DM increasing, T2DM has become a major public health concern. A study reported that ~425 million individuals worldwide were diagnosed with T2DM in 2017, which is expected to be ~629 million by 2045 (1). However, the most concerning part of T2DM is that a number of complications can arise over the prolonged course of the disease which seriously threaten human health, such as cardiovascular disease, retinopathy, neuropathy, and nephropathy (2). Diabetic kidney disease (DKD), the most frequent complication of diabetes mellitus (DM), has been reported to be the main cause of poor prognoses in DM patients (3,4). DKD is characterized by gradual renal dysfunction and fibrosis caused by glycolipid metabolism disorder and is the main cause of end-stage kidney disease (5). Of DM patients, ~30-40% have been reported to develop DKD (6,7), which has received increased attention due to the increase of T2DM patients and its difficult treatment (8,9). However, its pathogenesis is not fully clarified, therefore, exploring the mechanisms of T2DM-induced DKD and seeking potential therapeutic targets require further study.

Increasing evidence reveals that inflammation of the kidney plays a pivotal role in T2DM-induced DKD (10). The persistent hyperglycemic and hyperlipidemic environments in T2DM can cause renal inflammation and damage, eventually resulting in renal fibrosis (11). Inflammasomes are a multi-protein complex of intracytoplasmic pattern recognition receptors, which are reported to recognize damage- and pathogen-associated molecular patterns (12) and growing evidence suggests that inflammasomes may play a critical role in evoking inflammation by serving as a platform to recruit the apoptosis-associated speck-like protein containing a CARD (ASC) and procaspase-1, leading to the maturation of inflammatory cytokines (13). Nod-like receptor protein 3 (NLRP3) inflammasomes are reported to be involved in the occurrence and progression of several renal diseases,

including DKD (14). NLRP3 inflammasomes promote the release of the inflammatory cytokines, such as IL-1β, in the pathogenesis of DKD, inducing sustained inflammation and renal injury and promoting dysfunction and fibrosis of the kidney (14). Inhibiting NLRP3 inflammasomes improves renal function, attenuates glomerulosclerosis, interstitial fibrosis and inflammation and decreases TGF-β and phosphorylated (p-)SMAD2/3 expression in the kidney of mice with T2DM, thereby inhibiting renal fibrosis (15). However, the regulatory mechanisms of NLRP3 in T2DM-induced DKD remain to be elucidated.

Intracellular calcium ($[Ca^{2+}]_i$) overload due to various reasons is associated with the progression of DKD (16). The transient receptor potential channel 6 (TRPC6), a canonical non-selective cation channel with significant permeability to Ca^{2+}, is widely expressed in a number of tissues such as the brain and kidney (17,18). According to data from the Human Protein Atlas (https://www.proteinatlas.org/ENSG00000137672-TRPC6/tissue), TRPC6 mRNA and protein are widely expressed in human tissues, including the digestive system, muscle tissues and the urinary system, with *Trpc6* being more abundantly expressed in the kidney. In the kidney, TRPC6 is largely expressed in multiple cells, such as podocytes, tubular epithelial cells and glomerular mesangial cells (19-21). It has been reported that drastic increases of TRPC6-mediated $[Ca^{2+}]_i$ causes podocyte hypertrophy and foot process effacement, resulting in renal injury in DKD (19). TRPC6 inhibitors are reported to alleviate renal fibrosis in a unilateral ureteral obstruction mouse model (22). Calcineurin (CN) is a type of Ca^{2+}-dependent phosphatase (23) and is reported to participate in multiple cellular processes and signal pathways (24). As an important nuclear transcription factor, nuclear factor of activated T cells (NFAT) can be regulated by CN to regulate the expression of target genes (25). NFAT2 is extensively expressed in renal tissue and plays a pivotal role in promoting podocyte damages in DKD, while the inhibitor of NFAT, 11R-VIVIT, can reduce renal injury and renal fibrosis in DKD (26). However, the mechanism of TRPC6-CN-NFAT2 regulation of NLRP3 inflammasomes, eventually promoting renal injury and glomerular fibrosis in DKD, remains to be elucidated.

The present study hypothesized that *Trpc6* knockout might inhibit calcium overload and NFAT2 activation, thus alleviating renal injury and fibrosis in T2DM-induced DKD. To test this hypothesis, the roles of T2DM in renal fibrosis, renal damage and changes in CN-NFAT2 signaling and NLRP3 inflammasomes were observed in wild type mice (WT) mice. The present study also explored the effects of *Trpc6* knockout on the improvement of T2DM-induced DKD and the regulation of CN-NFAT2 signaling and NLRP3 inflammasomes. The findings provided a more comprehensive understanding of DKD and provided additional therapeutic targets for treatment of T2DM-induced DKD.

Materials and methods

Animals and treatment. In the present study, the *Trpc6* knockout (*Trpc6*$^{-/-}$) mice (C57BL/6J) were obtained by Suzhou Cyagen Biosciences (Suzhou) Inc. The genotype of *Trpc6*$^{-/-}$ homozygous mice was determined by PCR amplification and agarose gel electrophoresis separation (Fig. SI). WT mice were obtained from the same litter of *Trpc6*$^{-/-}$ mice. The mice were bred in an environmentally controlled room (temperature, 22-24˚C; relative humidity, 50-60%) under a 12-h light/dark cycle with unlimited access to food and water. After the acclimatization of 50 male mice (20-25 g) at 8 weeks of age, they were divided into five groups: WT, *Trpc6*$^{-/-}$, WT + high fat diet (HFD) + streptozotocin (STZ), *Trpc6*$^{-/-}$ + HFD and *Trpc6*$^{-/-}$ + HFD + STZ (n=10 per group). The mice of the WT and *Trpc6*$^{-/-}$ groups were fed with a growth-maintenance diet and the other mice were given a HFD of 20% carbohydrates, 20% protein and 60% fat (cat. no. D12492, Jiangsu Xietong Pharmaceutical Bio-engineering Co., Ltd.) for eight weeks.

After eight weeks, the mice of the WT + HFD + STZ and *Trpc6*$^{-/-}$ + HFD + STZ groups (fasting without water restriction for 8 h) were treated intraperitoneally with STZ (110 mg/kg, Shanghai Yuanye Bio-Technology Co., Ltd.), which was dissolved in a 0.1 M sodium citrate buffer to induce the T2DM model (27). The fasting blood glucose (FBG) level was measured after 72 h. Mice with a FBG concentration ≥16.7 mM were considered optimal for further experiments. Next, each group was given the same diet as described previously for eight weeks. The health and behavior of the animals were monitored daily. Throughout the experiment, one mouse in the *Trpc6*$^{-/-}$ + HFD + STZ group succumbed to infection at week 13 and one mouse in the WT + HFD + STZ group succumbed to hyperglycemia at weeks 13 and 14, respectively. The remaining mice were sacrificed. The mice were anesthetized using an intraperitoneal (IP) injection of tribromoethanol (300 mg/kg) and sacrificed by cervical dislocation after orbital blood extraction (once; ~0.2 ml) when they did not respond to gentle stimulation. All experiments were conducted under the approval of the Anhui Medical University Ethics Committee (approval no. LLSC20190302). When a click in the neck of the mouse was clearly heard, i.e., cervical spine detachment, spinal cord rupture and the heartbeat of the mouse stopped and the spontaneous respiration ceased it was considered that the mouse was dead and both kidneys were quickly removed. One kidney was fixed with paraformaldehyde (4%) for histological examination and the other was placed at -80˚C for western blot analysis.

Detection of body weight, FBG and biochemical parameters. The body weight and FBG levels were observed to evaluate the T2DM model. The body weight (n=8-10) was measured once every two weeks. The FBG levels were measured every two weeks from 8-16 weeks by using a portable blood glucose meter (Sinocare Inc.). The test was performed using a second drop of blood from the tail vein, the total blood volume being ~40 μl. Following the sacrifice of the mice, the serum creatinine (SCR) and blood urea nitrogen (BUN) were measured using urea assay kit and creatinine assay kit (Nanjing Jiancheng Bioengineering Institute; cat. nos. C013-2-1 and C011-2-1). At 16 weeks, the 24 h urine samples were collected and kits used as follows: the urinary albumin level (cat. no. C035-2-1), serum total cholesterol (TC; cat. no. A111-1-1), triglyceride (TG; cat. no. A110-1-1), free fatty acids (FFA; cat. no. A042-2-1), low density lipoprotein (LDL-C; no. A113-1-1) and high-density lipoprotein (HDL-C; cat. no. A112-1-1) (all Nanjing Jiancheng

Bioengineering Institute). All kit procedures were conducted strictly according to the manufacturer instructions.

Histology examination. The morphological examination of the kidneys was performed using hematoxylin and eosin (H&E), periodic acid-Schiff (PAS; Beijing Solarbio Science & Technology Co., Ltd.; cat. no. G1208) and Masson's trichrome staining (Beijing Solarbio Science & Technology Co., Ltd.; cat. no. G1340) methods. H&E staining was conducted to observe the pathological changes of the kidney (28). Briefly, the kidneys (n=4) were fully fixed with paraformaldehyde (4%) at 4˚C for 24 h, dehydrated and embedded in paraffin, then cut into 5-μm thick sections. The kidney sections were deparaffinized in xylene and rehydrated in graded alcohol series (anhydrous ethanol, 85% ethanol and 75% ethanol), and then stained with hematoxylin for 4 min and eosin for 35 sec at room temperature (RT). After being rinsed with running water, the tissues were sealed using neutral resin and were imaged using an Intelligent Tissue Section Imaging System (3DHISTECH, Ltd.) to observe renal histopathological changes. Renal injury was scored in a blinded manner with the following scoring criteria: no injury=0; <25%=1; 25-50%=2; 50-75%=3; and >75%=4.

Masson's staining was performed to observe tissue fibrosis (29). For Masson staining, the paraffin sections (n=4) were first dewaxed, hydrated and stained with hematoxylin for 4 min, then underwent acidic ethanol fractionation for 15 sec and were stained with Masson's blue solution for 5 min. This was followed by fuchsin staining for 9 min, phosphomolybdic acid for 3 min, then aniline blue staining for 6 min. All steps were performed at RT. The sections were then sealed using neutral resin and imaged using the Intelligent Tissue Section Imaging System (3DHISTECH, Ltd.). Finally, the mean density of Masson staining from five random areas (magnification, x400) per section was analyzed by the Image-pro Plus 6.0 image software (Media Cybernetics, Inc.) to evaluate renal fibrosis.

PAS staining was further performed to measure the disposition of acidic glycoproteins in order to assess renal injury (30). The renal paraffin sections (n=4) were dewaxed and hydrated, then stained in the Schiff solution for 8 min and the hematoxylin solution for 1 min at RT. The sections were sealed using neutral resin. The results of PAS-staining were imaged with the Intelligent Tissue Section Imaging System (3DHISTECH, Ltd.). The positive areas were purplish red and the cell nuclei were blue. To evaluate the extent of renal fibrosis, the mean intensity of positive mesangial cells and the ratio of mesangial area to glomerular (%) from five random areas (magnification, x400) per section were analyzed by the Image-Pro Plus 6.0 software (Media Cybernetics, Inc.).

Reactive oxygen species (ROS) measurement. Dihydroethidium (DHE) was used to measure ROS production (31). Briefly, mice (n=3) were injected via the tail vein with DHE (0.1 ml/10 g, 100 μM; Beyotime Institute of Biotechnology). The mouse was euthanized by cervical dislocation after 30 min and the kidneys were quickly removed and embedded in OCT composite media (Sakura Finetek USA, Inc.) at -20˚C for 1 h. The renal tissue was sectioned at 10 μm using a cryostat (CM3050; Leica Microsystems GmbH) and the sections rinsed three times with PBS buffer and stained with Hoechst solution (5 mg/l; MilliporeSigma) at RT for 5 min. The section was washed and sealed with an anti-fluorescent quenching agent, then imaged using the Intelligent Tissue Section Imaging System (3DHISTECH, Ltd.). Finally, the fluorescence intensity from three random areas (magnification, x400) per section was examined using the Image-Pro Plus software (Media Cybernetics, Inc.) to detect the levels of ROS production.

β-galactosidase (β-Gal) activity. The β-Gal activity was examined by β-Gal staining for senescence-associated injury. The frozen sections (n=3) were first warmed to RT, allowed to dry slightly, fixed with the β-Gal fixative (Beyotime Institute of Biotechnology) for 15 min, then washed three times with PBS. The PBS was then discarded and the β-Gal staining working solution was added to the sections for incubation at 37˚C overnight. The staining solution was then discarded, rinsed three times with PBS and imaged using the Intelligent Tissue Section Imaging System (3DHISTECH, Ltd.). Finally, the mean density (blue) from three random areas (magnification, x400) per tissue was examined with the Image-Pro Plus software (Media Cybernetics, Inc.) to estimate β-Gal activity.

Immunohistochemistry. The 5 μm paraffin sections of kidney tissue (n=4) were dewaxed and rehydrated. For antigen retrieval, the section was heated using a microwave oven for 8 min in sodium citrate buffer, stopped for 7 min, then reheated for 8 min. The section was then incubated in H_2O_2 (3%) at RT for 30 min to block endogenous peroxidase and then sealed with blocking solution at RT for 1 h. The sections were incubated in rabbit polyclonal antibodies (Table SI) at 4˚C overnight. The sections were rinsed with PBS and incubated with polymer-coupled peroxidase-labeled goat anti-rabbit IgG at RT for 1 h, then the section was stained with a DAB kit and hematoxylin. Finally, at the end of the light-protected sealing, the sections were imaged by the Intelligent Tissue Section Imaging System (3DHISTECH, Ltd.). The mean intensity from five random renal cortex regions (magnification, x400) per tissue was quantified by Image-Pro Plus software (Media Cybernetics, Inc.) to assess the expression of fibronectin (FN) and collagen IV (COL4).

Western blotting. Total proteins from renal cortexes (n=4) were isolated by the RIPA lysates buffer (cat. no. P0013B; Beyotime Institute of Biotechnology) in a fully automated sample freeze grinder (Shanghai Jingxin Industrial Development Co., Ltd.). After lysing for 30 min on ice, the tissue lysate was centrifuged (12,000 x g) at 4˚C for 20 min to extract the supernatant. The protein concentration was determined using a BCA assay kit, and then the protein (20 μg) was separated on 10% gels using SDS-PAGE and transferred onto PVDF membranes. Next, the membrane was blocked with the 5% defatted milk at RT for 1 h and was incubated in the primary antibodies (Table SI) at 4˚C overnight. The membrane was then washed three times in TBS with 0.05% Tween-20 (TBST) and was incubated in the corresponding secondary antibodies of goat anti-mouse IgG (cat. no. S0002; Affinity Biosciences; 1:10,000) or goat anti-rabbit IgG (cat. no. S0001; Affinity Biosciences; 1:10,000) for 1 h at RT. After being rinsed in TBST three times, the Western ECL kit (Bio-Rad Laboratories, Inc.) was applied to

visualize the results and the Chemi Imaging System (Q4800 mini, Bioshine Chemi) was used to image the bands. The intensity of protein bands was measured by an image J v1.53 software (National Institutes of Health). The results were normalized to β-actin to indicate the change in target protein.

Transmission electron microscopy. Briefly, the renal cortex specimen was sectioned into 1 mm^3 pieces and transferred to 2.5% glutaraldehyde at 4˚C for 2 h (n=3). After washing with PBS, the tissues were fixed with osmium tetroxide (1%) at RT for 2 h and embedded in Epon 812 for 12 h at 45˚C, and then heated at 72˚C for 24 h after dehydration. Ultrathin sections (70 nm) were sliced with an ultra-microtome (Leica UC7; Leica Microsystems GmbH). The section was double stained using lead citrate (stained for 30 min at RT) and uranyl acetate (stained at 4˚C overnight before embedding). Ultrastructural images were taken by a transmission electron microscope (HT7700; Hitachi High-Technologies Corporation). Glomerular ultrastructural damage was determined by observing the glomerular mesangial and foot processes.

Calcium imaging. The human mesangial cell (HMC) line was purchased from the Modern Analysis and Testing Center of Central South University. The HMC line was cultured with DMEM medium containing 10% FBS (Zhejiang Tianhang Biotechnology Co., Ltd.) and placed in a 37˚C incubator. The HMCs were divided into four groups: control, high glucose (HG; 25 mM) + palmitic acid (PA; 200 μM), vector + HG + PA and TRPC6-siRNA + HG + PA. The sequences of the short interfering RNAs (siRNAs) were: TRPC6 siRNA sense, 5'-GAG CAUCAUUGACGCAAAUTT-3' and antisense, 5'-AUUUGC GUCAAUGAUGCUCTT-3'; and negative control siRNA sense, 5'-UUCUCCGAACGUGUCACGUTT-3' and antisense, 5'-ACGUGACACGUUCGGAGAATT-3'. First, the cells were cultured in the dishes (35 mm) for 24 h and then transfected with Lipofectamine™ 2000 (Thermo Fisher Scientific, Inc.) with an empty vector or siRNA for 48 h at 37˚C according to the manufacturer's instructions. After treatment with PA and/or HG for 24 h, the HMCs were incubated in a Fura-2 AM dye solution with F-127 for 20 min at 37˚C and rinsed with an extracellular solution three times. The fluorescence density was detected every 3 sec under alternating excitation at 340 and 380 nm (F340 and F380) using a Digital Calcium Imaging Analysis Platform (IX73, DG-4PLUS/OF30; Olympus Corporation). The ratio (F340/F380) was measured with extracellular Ca^{2+} (1 mM) for 300 sec to estimate the basal level of $[Ca^{2+}]_i$. Then, the BAPTA (1 mM, MedChemExpress), a calcium chelator, or 2 mM $CaCl_2$ were added into the extracellular solution and the Δ ratio (F340/F380) was used to estimate the change of calcium homeostasis after BAPTA or high calcium stimulation. The experiment was repeated three times independently.

Nile red staining. Nile red staining was used to evaluate the production of lipids in the tissue sections. All steps were performed at room temperature. The frozen sections (n=3) were incubated in Nile red dilution (1 μg/ml) for 20 min. After rinsing three times, the sections were stained using Hoechst33258 for 4 min and were sealed using an anti-fluorescence quencher. All steps were performed at RT. The sections were imaged by the Intelligent Tissue Section Imaging System (3DHISTECH, Ltd.). The red fluorescence intensity from three renal cortex regions (magnification, x400) per section was quantified using Image-Pro Plus software (Media Cybernetics, Inc.) to evaluate the lipid production in mouse kidney cortical regions.

Statistical analysis. The experimental results in the present study are shown as mean ± SD of ≥3 independent experiments. For statistical analysis, the data was analyzed using the GraphPad Prism 9.0 statistical software (GraphPad; Dotmatics). Data from each group were analyzed first by one-way ANOVA, then the difference between the two groups was performed by Tukey's test. $P<0.05$ was considered to indicate a statistically significant difference.

Results

Trpc6 knockout improves renal function and blood lipid metabolism in T2DM mice. The results revealed that body weight increased slowly in both WT and *Trpc6*$^{-/-}$ groups, suggesting that *Trpc6* knockout had no obvious influence on body weight of normal mice. However, in *Trpc6*$^{-/-}$ + HFD mice, body weight significantly increased from 2-16 weeks compared with the WT control mice (Fig. S2A; $P<0.01$). The T2DM mice showed significant weight loss in both WT + HFD + STZ and *Trpc6*$^{-/-}$ + HFD + STZ groups after STZ injection, compared with the WT mice (Fig. S2A; $P<0.01$). Compared with the WT + HFD + STZ mice, *Trpc6* knockout visibly delayed body weight loss (Fig. S2A; $P<0.01$) in *Trpc6*$^{-/-}$ T2DM mice. The FBG results indicated that the FBG was raised in the *Trpc6*$^{-/-}$ + HFD mice compared with the WT control mice, but within the normal range. After STZ modeling, the FBG levels were raised in both WT + HFD + STZ and *Trpc6*$^{-/-}$ + HFD + STZ mice compared with the WT mice (Fig. S2B; $P<0.01$). However, compared with the WT + HFD + STZ mice, *Trpc6* knockout decreased the FBG levels (Fig. S2B; $P<0.01$) in T2DM mice, but the levels were still >20 mM. Additional renal function indexes showed that the levels of BUN, SCR and urine protein were clearly raised in WT + HFD + STZ mice compared with the WT mice (Fig. S2C-E; $P<0.05$ or $P<0.01$); however, compared with the WT + HFD + STZ mice, knockout *Trpc6* markedly decreased the levels of BUN, SCR and urine protein in T2DM mice (Fig. S2C-E; $P<0.05$). Furthermore, HFD-treatment alone had no influence on renal function in *Trpc6*$^{-/-}$ mice compared with the WT control mice. The results revealed that *Trpc6* knockout significantly improved renal function, but had only a weak hypoglycemic effect in T2DM mice.

The present study further evaluated the change of lipid metabolism-related parameters of FFA, TC, TG, LDL-C and HDL-C in serum and FFA in renal tissue. The results showed no significant difference in these parameters in *Trpc6*$^{-/-}$ mice compared with the WT mice, indicating that knockout *Trpc6* had no influence on lipid metabolism in normal mice. However, the levels of these parameters, were markedly raised in the WT + HFD + STZ mice, with the exception of HDL-C (Fig. S2F-K; $P<0.05$ or $P<0.01$). Compared with WT + HFD + STZ mice, *Trpc6* knockout clearly decreased the levels of TG, TC and LDL-C (Fig. S2F, J and I; $P<0.05$ or $P<0.01$) but there was no statistical difference in HDL-C and FFA in T2DM

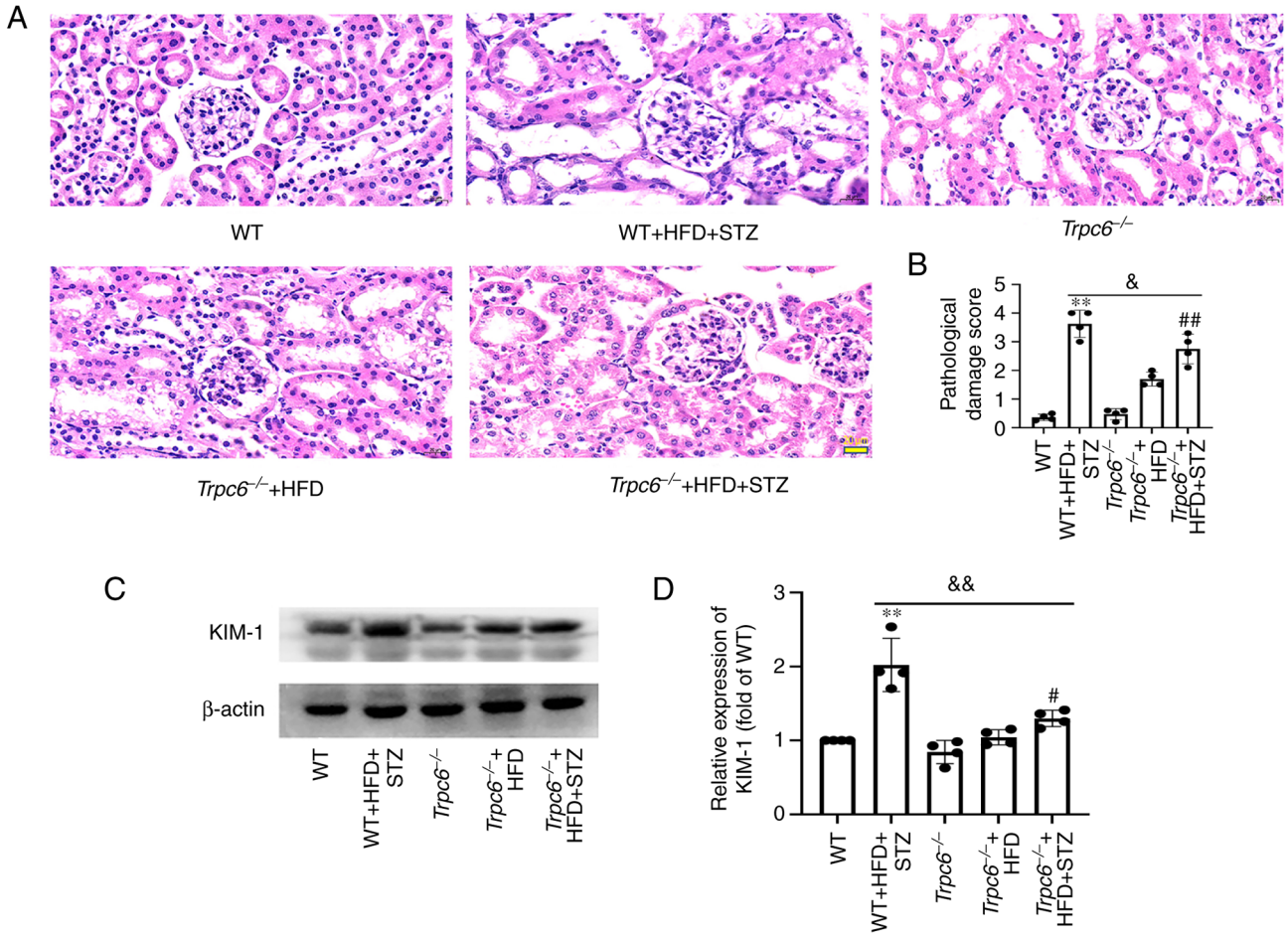

Figure 1. *Trpc6* knockout significantly protects against kidney injury and renal fibrosis in T2DM mice. (A) H&E staining (magnification, x400; scale bar, 20 μm); (B) The pathological scoring of kidney injury. (C) The bands of KIM-1 and β-actin; (D) Relative expression of KIM-1. Results are expressed as mean ± SD, n=4. **P<0.01 vs. WT group; $^{\#}$P<0.05 and $^{\#\#}$P<0.01 vs. *Trpc6*$^{-/-}$ group; $^{\&}$P<0.05 and $^{\&\&}$P<0.01 vs. WT + HFD + STZ group. T2DM, type-2 diabetes mellitus; H&E, hematoxylin and eosin; KIM-1, kidney injury molecule-1; WT, wild type; HFD, high fat diet; STZ, streptozotocin.

mice. The data indicated that *Trpc6* knockout may ameliorate blood lipid metabolism, but had no effect on FFA in renal tissues of T2DM mice.

Trpc6 knockout significantly protects against kidney injury and renal fibrosis in T2DM mice. The present study further explored renal injury by using H&E staining, immunoblotting and PAS staining in *Trpc6*$^{-/-}$ T2DM mice. The H&E staining indicated that there was no obvious renal injury in WT, *Trpc6*$^{-/-}$ and *Trpc6*$^{-/-}$ + HFD group non-T2DM mice. When compared with the WT mice, the renal tissue showed evident damages in WT + HFD + STZ mice; the glomerular mesangial cells were expanded and proliferated and a number of renal tubular cells were vacuolated and detached. However, these pathological changes were improved in *Trpc6*$^{-/-}$ + HFD + STZ mice (Fig. 1A and B; P<0.05). The present study further evaluated the biomarker, kidney injury molecule-1 (KIM-1), by western blotting (32). The results revealed that the expression of KIM-1 in the kidney of WT + HFD + STZ mice was clearly raised compared with WT mice (Fig. 1C and D; P<0.01), but was markedly reduced in *Trpc6*$^{-/-}$ + HFD + STZ mice compared with WT + HFD + STZ mice (Fig. 1C and D; P<0.01). PAS staining was used to assess glomerulosclerosis and renal damage (33). The PAS staining results revealed that more PAS-positive substances were found in the glomeruli and renal tubulointerstitial in WT + HFD + STZ mice compared with the WT mice (Fig. 2A-C; P<0.01). *Trpc6* knockout significantly alleviated PAS-positive substances in *Trpc6*$^{-/-}$ + HFD + STZ mice compared with WT + HFD + STZ mice (Fig. 2A-C; P<0.05). The results revealed that *Trpc6* knockout clearly protected against renal injury in T2DM mice.

Renal fibrosis is another important marker of renal damages. The present study used Masson staining to examine whether *Trpc6* knockout had protective effects on glomerular fibrosis in T2DM mice. The results indicated that little fibrosis was found in the renal tubules and glomeruli in the WT, *Trpc6*$^{-/-}$ and *Trpc6*$^{-/-}$ + HFD groups. Compared with the WT mice, the tubular interstitial and glomerular fibrosis (blue) was markedly increased in WT + HFD + STZ mice (Fig. 2A and D; P<0.01). By contrast, *Trpc6* knockout clearly alleviated renal fibrosis in *Trpc6*$^{-/-}$ + HFD + STZ mice compared with WT + HFD + STZ mice (Fig. 2A and D; P<0.05). The results revealed that knockout *Trpc6* may protect against renal fibrosis in T2DM mice and that HFD treatment alone had no influence on renal injury in *Trpc6*$^{-/-}$ mice.

Trpc6 knockout clearly improves the glomerular ultrastructure in T2DM mice. Transmission electron microscopy was performed to detect the effect of *Trpc6* knockout on the

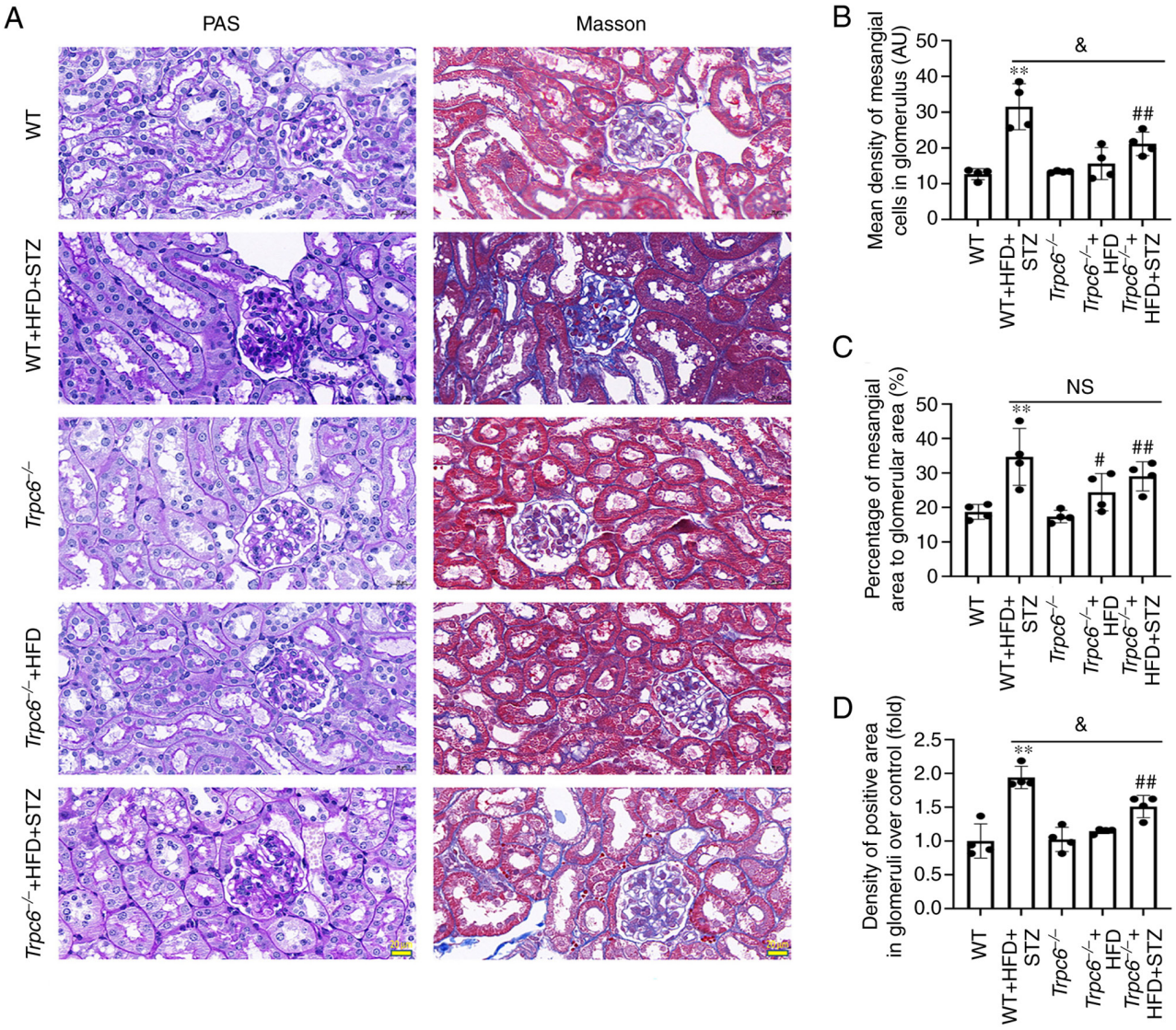

Figure 2. *Trpc6* knockout significantly protects against kidney injury and renal fibrosis in T2DM mice. (A) PAS and Masson staining (magnification, x400; scale bar, 20 μm); (B) The mean density of mesangial cells in the glomerulus; (C) The percentage of mesangial area to glomerular area; (D) The density of the positive area in glomeruli over control. Results are expressed as mean ± SD, n=4. **P<0.01 vs. WT group; $^{\#}$P<0.05 and $^{\#\#}$P<0.01 vs. *Trpc6*$^{-/-}$ group; $^{\&}$P<0.05 vs. WT + HFD + STZ group; NS, not significant. T2DM, type-2 diabetes mellitus; PAS, periodic acid-Schiff; WT, wild type; HFD, high fat diet; STZ, streptozotocin.

glomerular microstructure in T2DM mice. The results showed that there was almost no glomerular damage in WT, *Trpc6*$^{-/-}$ and *Trpc6*$^{-/-}$ + HFD group non-T2DM mice (Fig. 3). Compared with the WT control mice, the WT + HFD + STZ mice showed obvious glomerular ultrastructure damages. The foot processes showed obvious fusion and disappearance (Fig. 3). However, *Trpc6* knockout clearly improved these glomerular ultrastructure damages in *Trpc6*$^{-/-}$ + HFD + STZ mice when compared with WT + HFD + STZ mice (Fig. 3). The data indicate that *Trpc6* knockout clearly improves the glomerular ultrastructure in T2DM mice.

Trpc6 knockout has no influence on renal ROS generation in T2DM mice. ROS-induced oxidative stress injury plays a main role in DKD progression (34); therefore, ROS accumulation in the renal cortex was assessed using DHE staining. The results revealed that there was almost no ROS production in the renal cortex in the WT and *Trpc6*$^{-/-}$ mice. Compared with the WT mice, ROS production was clearly increased in both WT + HFD + STZ mice and *Trpc6*$^{-/-}$ + HFD + STZ mice (Fig. 4A and B; P<0.01). Similarly, ROS production was also slightly raised in *Trpc6*$^{-/-}$ + HFD mice (Fig. 4A and B; P<0.01). These data indicated that knockout *Trpc6* showed no influence on the production of ROS in the renal cortex of T2DM mice and that ROS may be an upstream regulator of TRPC6 in T2DM.

Trpc6 knockout decreases β-Gal activity in T2DM mice. β-Gal is one of the essential markers of cellular senescence and is also involved in the pathogenesis of renal fibrosis (35). The present study developed a β-Gal staining to assess renal senescence in T2DM mice. The results revealed that there was only a small amount of β-Gal expression in the WT and *Trpc6*$^{-/-}$ groups. Compared with WT mice, the expression of β-Gal was clearly increased in WT + HFD + STZ mice (Fig. S3A and B; P<0.01). The activities of β-Gal were also increased in *Trpc6*$^{-/-}$ + HFD mice when compared with *Trpc6*$^{-/-}$ mice (Fig. S3A and B;

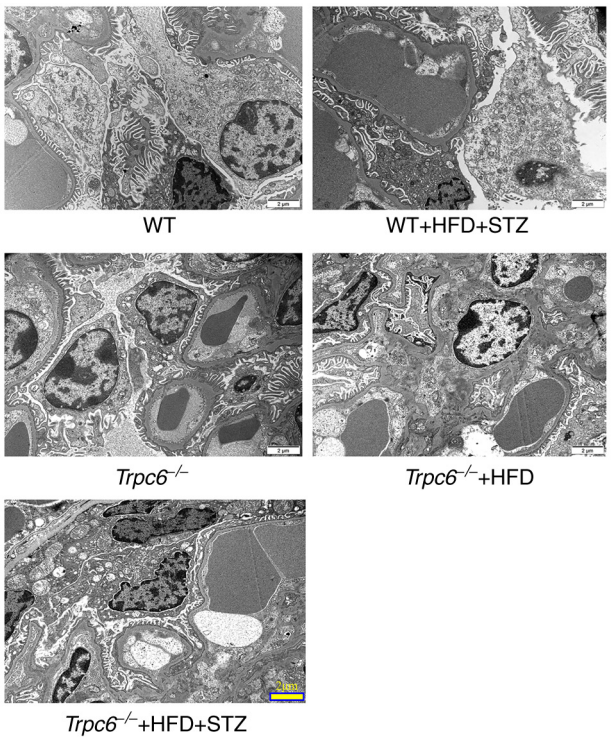

Figure 3. *Trpc6* knockout clearly improves the glomerular ultrastructure in T2DM mice (transmission electron microscopy; magnification, x10,000; scale bar, 2 μm). T2DM, type-2 diabetes mellitus; WT, wild type; HFD, high fat diet; STZ, streptozotocin.

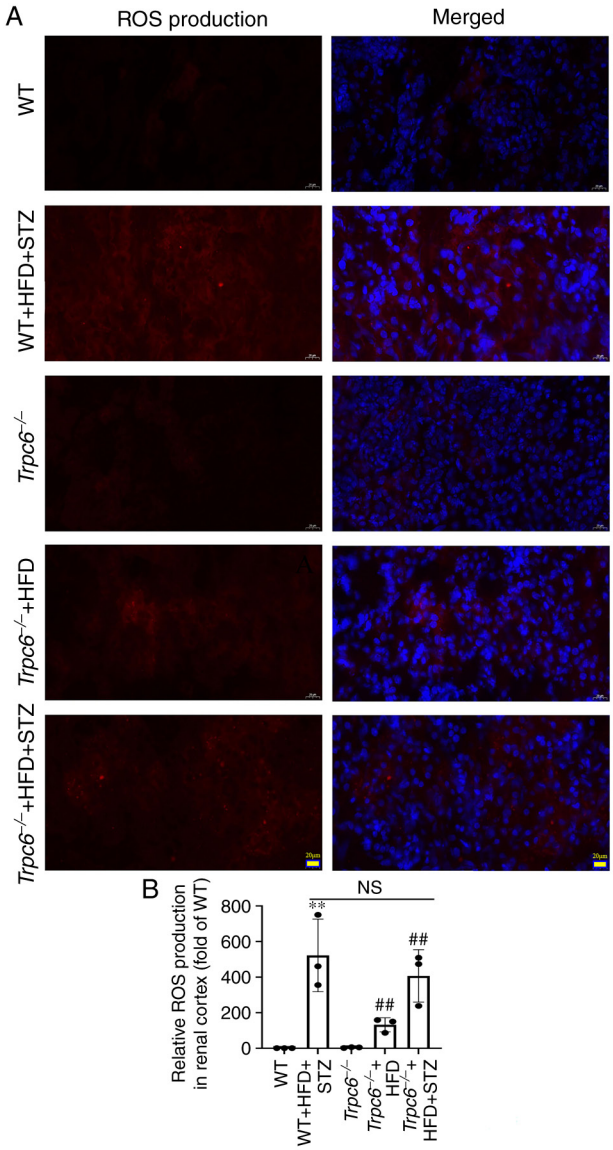

Figure 4. *Trpc6* knockout has no influence on renal ROS generation in T2DM mice. (A) The production of ROS in the renal cortex (DHE staining, magnification, x400; scale bar, 20 μm); (B) Relative ROS production in renal cortex. Results are expressed as mean ± SD, n=4. **P<0.01 vs. WT group; $^{\#\#}$P<0.01 vs. *Trpc6*$^{-/-}$ group; NS, not significant. ROS, reactive oxygen species; T2DM, type-2 diabetes mellitus; DHE, dihydroethidium; WT, wild type; HFD, high fat diet; STZ, streptozotocin.

P<0.01). However, the activities of β-Gal were clearly reduced in *Trpc6*$^{-/-}$ + HFD + STZ mice when compared with WT + HFD + STZ mice (Fig. S3A and B; P<0.01). These results indicated that knockout of *Trpc6* improved renal aging injury in T2DM mice.

Trpc6 knockout decreases renal fibrosis-related protein expression in T2DM mice. To confirm the role of *Trpc6* knockout in renal fibrosis in T2DM mice, the expression of the COL4 and FN genes were measured using immunohistochemistry (36). The results demonstrated that the expression of COL4 and FN were clearly increased in the kidney of WT + HFD + STZ mice when compared with WT mice (Fig. 5A-C; P<0.01) and the expression of COL4 and FN were clearly reduced in the *Trpc6*$^{-/-}$ + HFD + STZ mice compared with WT + HFD + STZ mice (Fig. 5A-C; P<0.05 or P<0.01). The results indicated that knockout *Trpc6* can alleviate renal fibrosis in T2DM-induced DKD.

In addition, the levels of TGF-β and p-SMAD2/3 proteins were examined in T2DM mice. The results showed that the levels of TGF-β and p-SMAD2/3 were clearly raised in WT + HFD + STZ mice when compared with WT control mice (Fig. 6A, B and D; P<0.01); however, the expression of p-SMAD2/3 and TGF-β were clearly decreased in the *Trpc6*$^{-/-}$ + HFD + STZ mice when compared with WT + HFD + STZ mice (Fig. 6A, B and D; P<0.05). The results indicated that knockout of *Trpc6* may attenuate renal fibrosis by inhibiting the pathway of TGF-β/SMAD2/3in T2DM mice.

Trpc6 knockout decreases renal NLRP3 inflammasomes in T2DM mice. Next, NLRP3 inflammasomes in the kidney were measured to investigate whether *Trpc6* knockout can attenuate renal inflammation in T2DM mice. The results revealed that expression of NLRP3, cleaved-caspase-1 (P20) and ASC were clearly raised in the renal cortex of WT + HFD + STZ mice when compared with WT mice (Fig. 7A-D; P<0.01). However, *Trpc6* knockout clearly decreased the expression of NLRP3, caspase-1 and ASC in *Trpc6*$^{-/-}$ + HFD + STZ mice when compared with WT + HFD + STZ mice (Fig. 7A-D; P<0.01 or P<0.05). The results suggested that T2DM promoted renal inflammation and that *Trpc6* knockout attenuated renal inflammation by inhibiting NLRP3 inflammasomes in T2DM.

Trpc6 knockout has no influence on CD36 and p-phospholipase C (PLC) expression and renal lipid deposition in T2DM mice. The effect of *Trpc6* knockout on CD36 and p-PLC expression in T2DM mice was evaluated. The results revealed that CD36

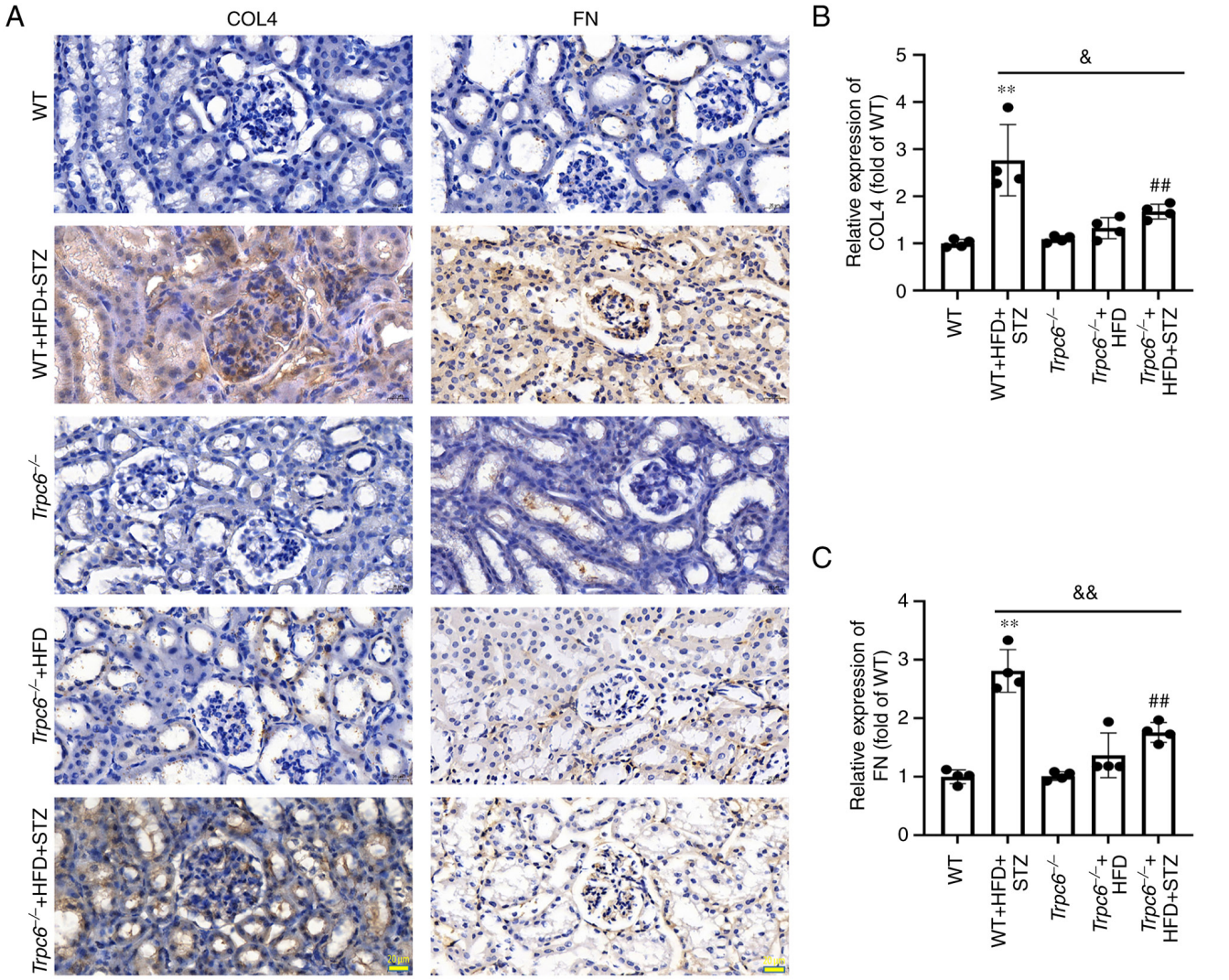

Figure 5. *Trpc6* knockout decreases renal fibrosis-related protein expression in T2DM mice. (A) Immunohistochemical staining (magnification, x400; scale bar, 20 μm); (B) Relative expression of COL4; (C) Relative expression of FN. Results are expressed as mean ± SD, n=4. **P<0.01 vs. WT group; $^{\#\#}$P<0.01 vs. *Trpc6*$^{-/-}$ group; $^{\&}$P<0.05 and $^{\&\&}$P<0.01 vs. WT + HFD + STZ group. T2DM, type-2 diabetes mellitus; COL4, collagen IV; FN, fibronectin; WT, wild type; HFD, high fat diet; STZ, streptozotocin.

and p-PLC expression was markedly upregulated in the kidney of WT + HFD + STZ mice and *Trpc6*$^{-/-}$ + HFD + STZ mice when compared with WT control mice (Fig. S4A-D; P<0.01 or P<0.05). Compared with the WT + HFD + STZ mice, knockout *Trpc6* had no significant influence on the levels of CD36 and p-PLC/PLC in renal cortex tissues of T2DM mice (Fig. S4A-D; P>0.05). The results suggest that the CD36 and PLC signaling may be the upstream regulator of TRPC6 in T2DM mice.

Nile red staining was used to assess the amount of lipid deposition in kidney. The results revealed that the renal lipid deposition in WT + HFD + STZ mice and *Trpc6*$^{-/-}$ + HFD + STZ groups was markedly increased when compared with WT control mice (Fig. S5A and B; P<0.01) and that knockout *Trpc6* shows no significant influence on renal lipid deposition in T2DM mice. Similarly, HFD-treatment alone also increased renal lipid deposition in *Trpc6*$^{-/-}$ + HFD mice (Fig. S5A and B; P<0.01). These data indicated that knockout *Trpc6* has no significant effect on the renal lipid deposition in T2DM mice and that lipid deposition may be the upstream regulator of TRPC6 in T2DM.

Trpc6 knockout inhibits the renal CN-NFAT2 signaling in T2DM mice. Next, changes in CN-NFAT2 signaling in *Trpc6*$^{-/-}$ T2DM was detected mice. The results revealed that there was a slight expression of TRPC6 in the kidney cortex of WT mice, but that TRPC6 expression was markedly increased in the kidneys of WT + HFD + STZ mice when compared with WT control mice (Fig. 8A and B; P<0.01). Additionally, TRPC6 was almost absent in kidney tissues of *Trpc6*$^{-/-}$ mice, *Trpc6*$^{-/-}$ + HFD mice and *Trpc6*$^{-/-}$ + HFD + STZ mice. Furthermore, the results indicated that CN and NFAT2 expression was markedly increased in the kidneys of WT + HFD + STZ mice when compared with WT control mice (Fig. 8A and B; P<0.01); however, *Trpc6* knockout clearly decreased CN and NFAT2 expression in the kidney of *Trpc6*$^{-/-}$ + HFD + STZ mice when compared with WT + HFD + STZ mice (Fig. 8A and B; P<0.05). The results indicated that TRPC6-CN-NFAT2 signaling may play a key role in promoting DKD in T2DM and that *Trpc6* knockout can partially inhibit the CN-NFAT2 signaling pathway in mice of T2DM.

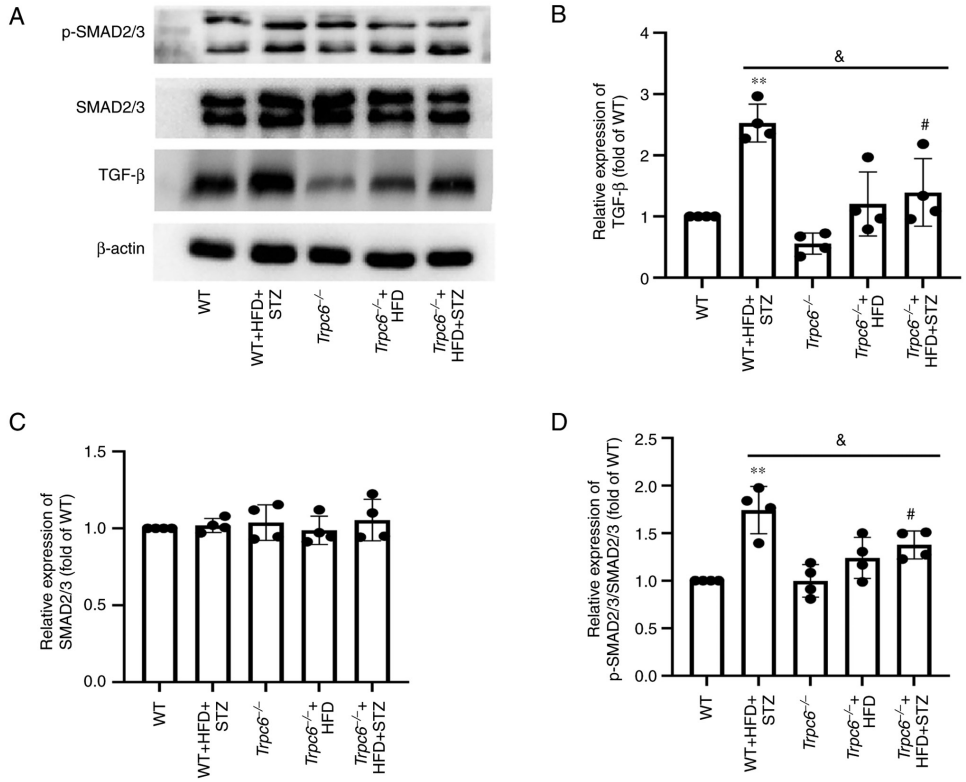

Figure 6. *Trpc6* knockout decreases the renal expressions of TGF-β and p-SMAD2/3 in T2DM mice. (A) The bands of TGF-β, SMAD2/3, p-SMAD2/3 and β-actin; (B) Relative expression of TGF-β; (C) Relative expression of SMAD2/3; (D) Relative expression of p-SMAD2/3/SMAD2/3. Results are expressed as mean ± SD, n=4. **P<0.01 vs. WT group; $^{\#}$P<0.05 vs. *Trpc6*$^{-/-}$ group; $^{\&}$P<0.05 vs. WT + HFD + STZ group; p-, phosphorylated; T2DM, type-2 diabetes mellitus; WT, wild type; HFD, high fat diet; STZ, streptozotocin.

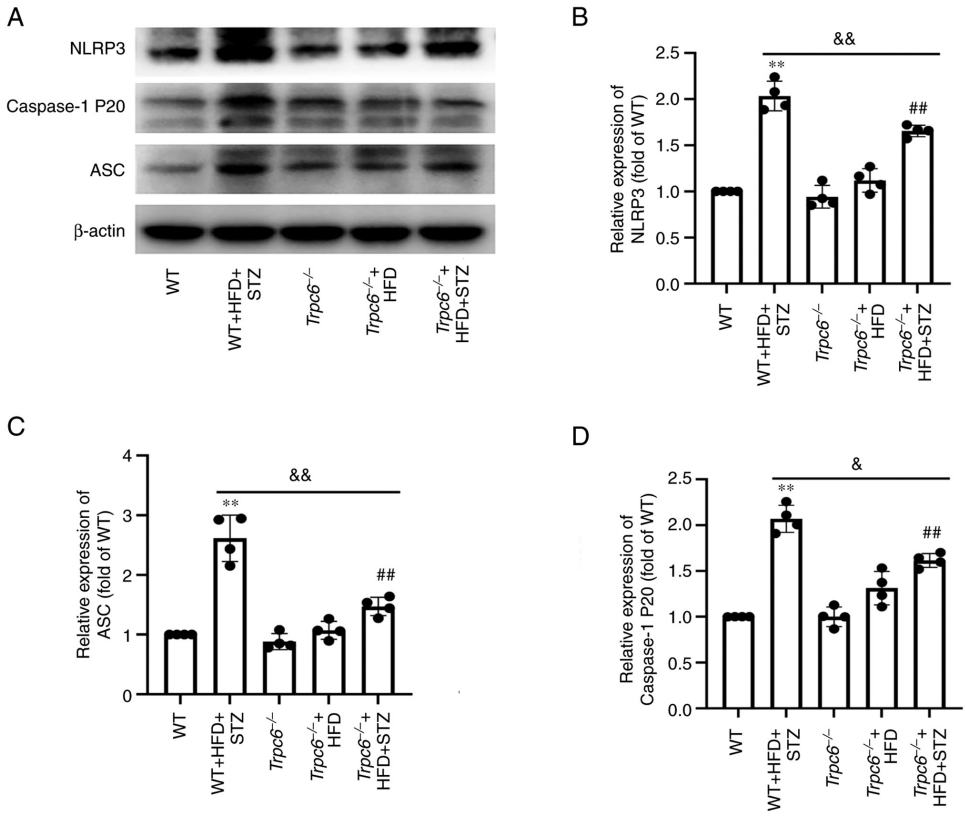

Figure 7. *Trpc6* knockout decreases renal NLRP3 inflammasomes in T2DM mice. (A) The bands of NLRP3, Caspase-1 p20, ASC and β-actin; (B) Relative expression of NLRP3; (C) Relative expression of ASC; (D) Relative expression of Caspase-1 p20. Results are expressed as mean ± SD, n=4. **P<0.01 vs. WT group; $^{\#\#}$P<0.01 vs. *Trpc6*$^{-/-}$ group; $^{\&}$P<0.05 and $^{\&\&}$P<0.01 vs. WT + HFD + STZ group. NLRP3, Nod-like receptor protein 3; T2DM, type-2 diabetes mellitus; WT, wild type; HFD, high fat diet; STZ, streptozotocin; ASC, apoptosis-associated speck-like protein containing a CARD.

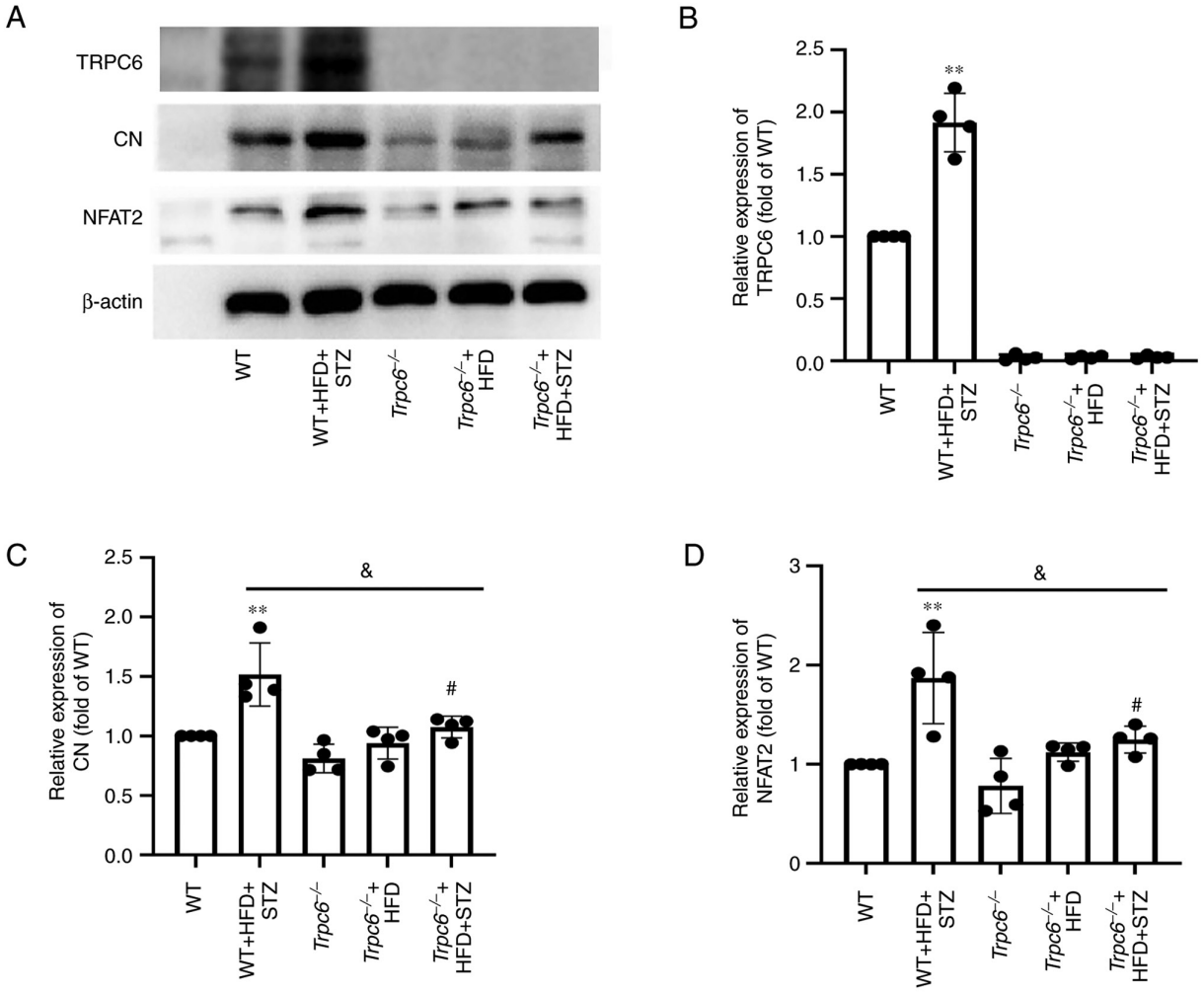

Figure 8. *Trpc6* knockout inhibits the renal CN-NFAT2 signaling in T2DM mice. (A) The bands of NFAT2, CN, TRPC6 and β-actin; (B) Relative expression of TRPC6; (C) Relative expression of CN; (D) Relative expression of NFAT2. Results are expressed as mean ± SD, n=4. **P<0.01 vs. WT group; $^{\#}$P<0.05 vs. *Trpc6*$^{-/-}$ group; $^{\&}$P<0.05 vs. WT + HFD + STZ group. CN, calcineurin; NFAT, nuclear factor of activated T cells; T2DM, type-2 diabetes mellitus; TRPC6, transient receptor potential channel 6; WT, wild type; HFD, high fat diet; STZ, streptozotocin.

Trpc6 knockout alleviates calcium homeostasis disorder in PA + HG-induced HMCs. Finally, the effects of *Trpc6* knockdown on $[Ca^{2+}]_i$ was evaluated by using calcium imaging in PA + HG-induced HMCs. The results revealed that the HMCs exhibited a significant calcium overload after PA + HG stimulation with $[Ca^{2+}]_i$ increase and calcium homeostasis imbalance after BAPTA and $CaCl_2$ stimulation, compared with the control group (Fig. 9A-D; P<0.01 or P<0.05). As compared with the PA + HG group, treatment with TRPC6-siRNA decreased the $[Ca^{2+}]_i$ and reduced the Δ Ratio F340/F380 induced by BAPTA and $CaCl_2$ stimulation (Fig. 9A-D; P<0.01 or P<0.05). These results indicated that PA + HG treatment can activate the TRPC6 channels in HMCs and that *Trpc6* knockdown can ameliorate the dysregulation of calcium homeostasis induced by PA + HG.

Discussion

T2DM is a common metabolic disease that is characterized by chronic disorder of glycolipid metabolism (37). DKD is the most dangerous complication caused by DM disorders. However, the pathogenesis of T2DM-induced DKD has not been fully elucidated and there are still no effective therapeutic methods for it. Some studies have reported that DKD involves multiple mechanisms, such as disruption of glucolipid metabolism, oxidative stress, inflammation, apoptosis, necrosis and autophagy (38-42). Recent evidence suggests that alterations in Ca^{2+} signaling can directly or indirectly influence the onset and progression of DKD (43). The TRPC6 channel is reported as a critical contributor in a number of renal diseases, including DKD (44,45), therefore, it was hypothesized that upregulation of TRPC6 in T2DM may regulate CN-NFAT2 signaling and activate NLRP3 inflammasomes and the TGF-β/p-SMAD2/3 pathway, resulting in renal damage and fibrosis. The present study found that knockout *Trpc6* clearly alleviated renal dysfunction, renal injury and fibrosis and inhibited CN-NFAT2 signaling and NLRP3 inflammasomes in T2DM mice. The present study suggested that *Trpc6* knockout can attenuate T2DM-induced DKD progression and that the TRPC6-CN-NFAT2 signaling pathway may be an important therapeutic target in DKD.

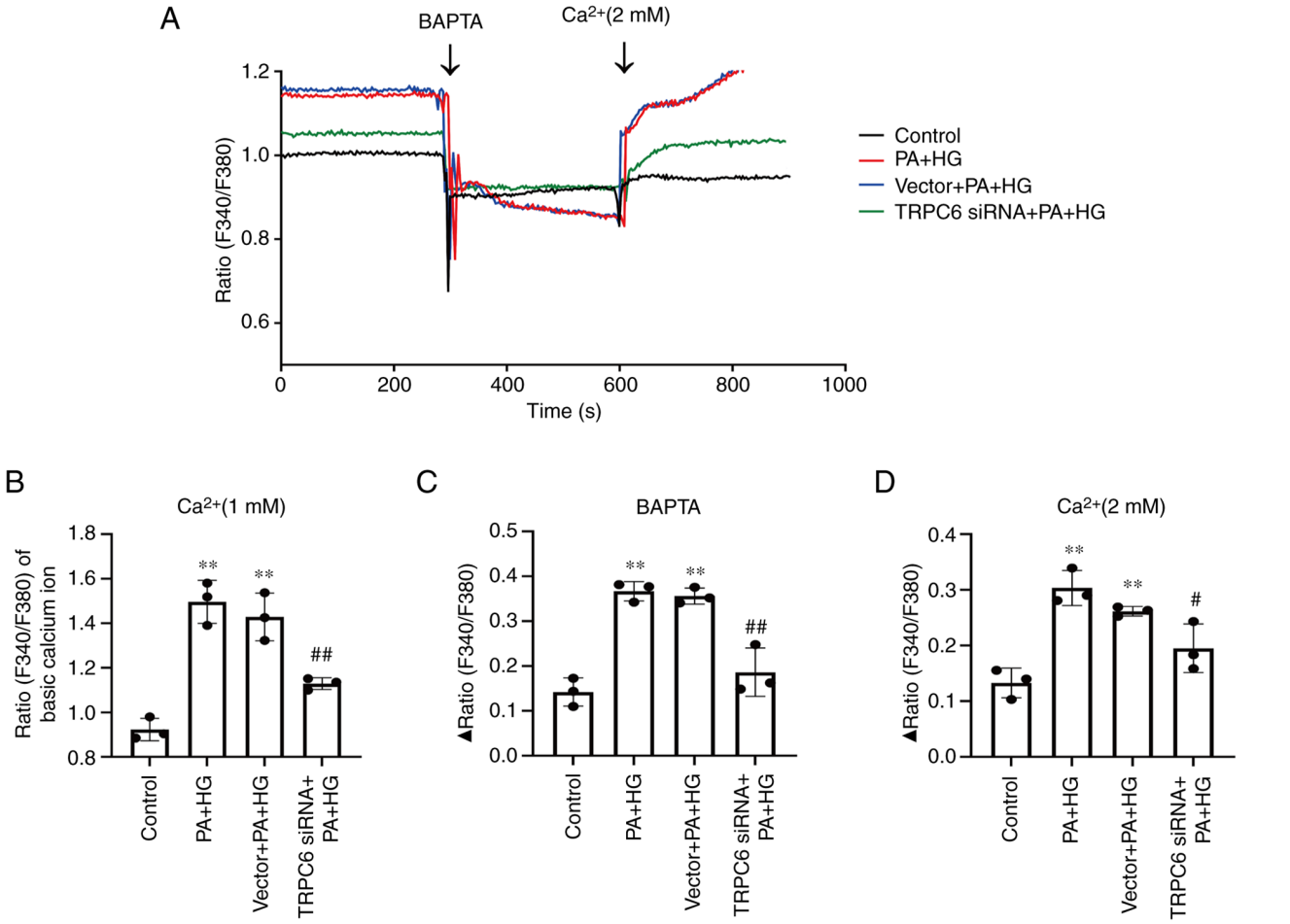

Figure 9. *Trpc6* knockout alleviates calcium homeostasis disorder in PA + HG-induced HMCs. (A) The ratio (F340/F380) corresponds to BAPTA and $CaCl_2$ (2 mM) in HMCs. (B) The ratio (F340/F380) of basal $[Ca^{2+}]_i$. (C) The ΔRatio (F340/F380) after BAPTA. (D) The ΔRatio (F340/F380) after $CaCl_2$. Data are expressed as mean ± SD, n=3. **P<0.01 vs. Control group; $^{\#}$P<0.05 and $^{\#\#}$P<0.01 vs. PA + HG group. PA, palmitic acid; HG, high glucose; HMCs, human mesangial cells.

The typical symptoms of T2DM are polydrinking, polyphagia, polyuria, weight loss and elevated fasting glucose (46), consistent with the results of body weight and FBG in the present study, demonstrating the success of the T2DM mice model. The SCR and BUN levels are important indicators for renal dysfunction assessment (47). In the present study, *Trpc6* knockout only had a slight hypoglycemic effect, but significantly reduced the serum BUN and SCR in T2DM mice, suggesting that *Trpc6* knockout can improve DKD in T2DM, but that it might not be caused by a hypoglycemic effect. Abnormal lipid metabolism is also an important feature of T2DM□therefore, the lipid metabolism in *Trpc6*$^{-/-}$ T2DM mice was further observed. The data indicated that the serum TG, TC, LDL-C, FFA and renal lipid deposition were markedly increased in WT T2DM mice. However, *Trpc6* knockout markedly reduced the serum TG, TC and LDL-C levels, but had no significant difference in FFA levels and lipid deposition in the renal cortex, suggesting that *Trpc6* knockout may have a mild regulation of lipid metabolism in the body, but has no influence on abnormal lipid metabolism in the kidney in T2DM. Mesangial cell expansion and the excessive deposition of acidic glycoprotein are important pathological features of DKD (48). In addition, the kidney injury factor, KIM-1, is often used to estimate renal injury (47). Moreover, the senescence-associated β-Gal, a marker of cellular senescence in response to cellular stress, is also often used to evaluate renal damages in DKD (49). It has been reported that diabetes and cellular senescence can induce a vicious cycle, resulting in the development of T2DM (50). In the present study, H&E and PAS staining results further confirmed that *Trpc6* knockout can attenuate renal injury and excessive deposition of acidic glycoprotein in T2DM mice. The KIM-1 and β-Gal results also confirmed that knockout of *Trpc6* clearly alleviated T2DM-induced renal injury and cellular senescence. Additionally, the electron microscope results revealed that *Trpc6* knockout significantly attenuated glomerular ultrastructure damages. These data suggested that knockout *Trpc6* can alleviate T2DM-induced renal injury.

Renal fibrosis, the most common pathological process in DKD, is a result of ongoing renal tissue damage and inflammation induced by hyperglycemic and hyperlipidemic environments in T2DM. Renal fibrosis, similar to other organs, is characterized by excessive extracellular matrix deposition, resulting in destruction of renal structure and reduction of renal function (51,52). Increased expression of FN and COL4 is largely involved in renal fibrosis (36); therefore, Masson staining is commonly used to examine collagen deposition in renal tissues (53). As shown by Masson staining and IHC results,

a significant increase of glomerular and interstitial fibrosis and FN and COL4 expression was observed in the T2DM mice, which was significantly attenuated by *Trpc6* knockout. The present study further indicated that *Trpc6* knockout significantly inhibited TGF-β/p-SMAD2/3 signaling, the primary pathogenic mechanism of glomerular fibrosis in DKD, which is highly activated in T2DM mice (54-57). Furthermore, HFD-treatment alone could not induce renal fibrosis in *Trpc6*$^{-/-}$ mice. These data suggested that *Trpc6* knockout can ameliorate renal fibrosis in T2DM. Additionally, the results indicated that knockout of *Trpc6* had no influence on lipid deposition and FFA in renal tissue and only had a slight hypoglycemic effect in T2DM mice. Accordingly, it was hypothesized that *Trpc6* knockout might improve T2DM-induced DKD through other mechanisms.

Previous studies suggested that Ca^{2+} homeostasis dysregulation is strongly associated with renal inflammation and injury (58) and that hyperglycemic and hyperlipidemic environments may significantly increase Ca^{2+} levels because of increased calcium entry into the cells (43,59). As the primary mechanism of Ca^{2+} influx, TRPC constitute a nonselective cation channel superfamily with Ca^{2+} permeability. Among the TRP family, TRPC6 is the most apparent calcium-selective channel and acts as an important calcium entry mechanism in the kidney. It has been reported that activation of TRPC6 due to increased gene expression or functionally acquired mutations can lead to heart and kidney disease (60,61). Under stress conditions, extracellular signaling molecules, in conjunction with G protein-coupled receptors, can activate PLCs on the plasma membrane, thereby cleaving phosphatidylinositol (4,5) biphosphate (PIP2) to generate the IP3 and DAG, which can increase intracellular Ca^{2+} by activating TRPC6 in the cell membrane, leading to intracellular calcium overload (62). In T2DM, abnormal lipid metabolism can lead to excessive FFA entering cells through CD36, a specific transport receptor, resulting in the activation of PLC and increase of DAG and IP3 (63). Calcium overload further activates CN-NFAT signaling, which triggers the pathological renal fibrotic disease. It has been reported that TRPC6 cation conductance is closely associated with calcium-dependent activation of CN and stimulates transcriptional regulation of NFAT2 (64-67). Meanwhile, NFAT2 is a downstream signaling molecule of the Ca^{2+} signaling pathway, but activation of NFAT2 itself can enhance the expression of the *Trpc6* gene to form a positive feedback loop (68). In addition, the damage and fibrosis of MCs are important pathological features of DKD. HMCs are often used as a cellular model for DKD (69). Our previous findings suggested that inhibition of *Trpc6* by SKF96365 (TRPC6 inhibitor) or siRNA could significantly suppress calcium homeostasis imbalance and significantly inhibit NFAT2 expression in the nucleus of PA-induced HMCs (68). In the present study, the results revealed that the CD36 and p-PLC levels were markedly increased in the T2DM mice. However, knockout of *Trpc6* had no influence on CD36 and p-PLC expression, which may be the upstream regulator of TRPC6 signaling in the T2DM mice. Furthermore, the results revealed that T2DM could increase the expression of TRPC6, CN and NFAT2 in renal tissue, which were clearly downregulated in *Trpc6*$^{-/-}$ T2DM mice. Calcium imaging results showed that knockdown of *Trpc6* by siRNA also significantly inhibited calcium homeostasis imbalance in PA + HG-induced HMCs. The results suggested that TRPC6-mediated activation of CN-NFAT2 signaling can facilitate the process of DKD and that *Trpc6* knockout may ameliorate renal injury and glomerular fibrosis by inhibiting calcium overload and the CN-NFAT2 pathway in T2DM mice.

Activation of CN-NFAT2 is closely related to the inflammatory cascade response (70), which is also one of the important pathogeneses of DKD. Accumulating evidence indicates that activation of NLRP3 inflammasomes can recruit the ASC and procaspase-1 to cleave the pro-IL-1β to the bioactive form, promoting the inflammatory cascade response in a number of diseases, including DKD (15). Studies revealed that activation of NLRP3 inflammasomes could exacerbate renal fibrosis in a number of kidney diseases (71,72). Inhibition of NLRP3 displayed anti-inflammatory effects and decreased renal injury and fibrosis in DKD (15). In the present study, the results suggested a significant activation of NLRP3 inflammasomes in T2DM mice and that knockout of *Trpc6* significantly inhibited the NLRP3 activation in the kidney of T2DM mice. These data suggested that NLRP3 signaling may be the downstream process of TRPC6-CN-NFAT2 signaling in DKD, however, the regulatory mechanism of NFAT2 on NLRP3 needs to be further studied.

Additionally, ROS plays a key role in the pathogenesis of renal injury and fibrosis, as excessive ROS production is associated with a number of pathophysiological processes, such as inflammation, cellular structure and Ca^{2+} homeostasis imbalance (73). The present study also demonstrated that ROS production in renal cortex was clearly elevated in T2DM mice; however, *Trpc6* knockout did not alleviate ROS production in T2DM mice, suggesting that the TRPC6-associated calcium homeostasis dysregulation might be the downstream signaling pathway of ROS oxidative stress.

In summary, T2DM can activate the CN-NFAT2 signaling pathway through a TRPC6-mediated calcium overload, leading to NLRP3 inflammasome activation and ultimately resulting in renal inflammation injury and renal fibrosis. *Trpc6* knockout inhibited the TGF-β/p-SMAD2/3 by suppressing renal calcium overload and CN-NFAT2 signaling and attenuating glomerular fibrosis in T2DM. However, the present study only explored the role of *Trpc6* knockout in improving DKD *in vivo*. It is remains to be elucidated what the relationship of TRPC6 and NLRP3 is and future studies are needed to investigate the mechanism of TRPC6 in DKD progression.

Acknowledgements

The authors would like to thank Miss Hanyang Xu, Mr. Bo Li and Mr. Dake Huang (School of Basic Medical Sciences, Anhui Medical University, Anhui, China) for providing technical assistance.

Funding

The present study was supported by the National Natural Science Foundation of China (grant nos. 81970630 and 82204703), the Natural Science Foundation of Anhui Province (grant no. 2208085MH219) and the Major Projects of the Anhui Provincial Department of Education (grant no. KJ2020ZD14).

Availability of data and materials

The datasets used and analyzed during the present study are available from the corresponding author on reasonable request.

Authors' contributions

RS performed the experiments, and prepared the manuscript. MH and YL contributed to the immunoblot analysis and interpretation of the results. QFS and YS collated the data. LH and LLK were mainly responsible for the histological experiments. WPL and WZL designed the study, critically revised the manuscript for intellectually important content and supervised the study. WPL and WZL confirm the authenticity of all the raw data. All authors read and approved the final manuscript.

Ethics approval and consent to participate

All experiments involving animals were approved by the Anhui Medical University Ethics Committee (approval no. LLSC20190302).

Patient consent for publication

Not applicable.

Competing interest

The authors declare that they have no competing interests.

References

1. Toi PL, Anothaisintawee T, Chaikledkaew U, Briones JR, Reutrakul S and Thakkinstian A: Preventive role of diet interventions and dietary factors in type 2 diabetes mellitus: An umbrella review. Nutrients 12: 2722, 2020.
2. Iatcu CO, Steen A and Covasa M: Gut microbiota and complications of type-2 diabetes. Nutrients 14: 166, 2021.
3. KDOQI clinical practice guideline for diabetes and CKD: 2012 update. Am J Kidney Dis 60: 850-886, 2012.
4. Jia Y, Guan M, Zheng Z, Zhang Q, Tang C, Xu W, Xiao Z, Wang L and Xue Y: miRNAs in urine extracellular vesicles as predictors of early-Stage diabetic nephropathy. J Diabetes Res 2016: 7932765, 2016.
5. Ma R, Wang Y, Xu Y, Wang R, Wang X, Yu N, Li M and Zhou Y: Tacrolimus protects podocytes from apoptosis via downregulation of TRPC6 in diabetic nephropathy. J Diabetes Res 2021: 8832114, 2021.
6. Adeshara KA, Diwan AG and Tupe RS: Diabetes and complications: Cellular signaling pathways, current understanding and targeted therapies. Curr Drug Targets 17: 1309-1328, 2016.
7. Gregg EW, Sattar N and Ali MK: The changing face of diabetes complications. Lancet Diabetes Endocrinol 4: 537-547, 2016.
8. Ali MK, Pearson-Stuttard J, Selvin E and Gregg EW: Interpreting global trends in type 2 diabetes complications and mortality. Diabetologia 65: 3-13, 2022.
9. Caro JJ, Ward AJ and O'Brien JA: Lifetime costs of complications resulting from type 2 diabetes in the U.S. Diabetes Care 25: 476-481, 2002.
10. Rayego-Mateos S, Rodrigues-Diez RR, Fernandez-Fernandez B, Mora-Fernández C, Marchant V, Donate-Correa J, Navarro-González JF, Ortiz A and Ruiz-Ortega M: Targeting inflammation to treat diabetic kidney disease: The road to 2030. Kidney Int 103: 282-296, 2023.
11. Karunasagara S, Hong GL, Park SR, Lee NH, Jung DY, Kim TW and Jung JY: Korean red ginseng attenuates hyperglycemia-induced renal inflammation and fibrosis via accelerated autophagy and protects against diabetic kidney disease. J Ethnopharmacol 254: 112693, 2020.
12. Gong Z, Zhao S, Zhou J, Wang L, Du X, Li H, Chen Y, Cai W and Wu J: Curcumin alleviates DSS-induced colitis via inhibiting NLRP3 inflammsome activation and IL-1β production. Mol Immunol 104: 11-19, 2018.
13. Sharma BR and Kanneganti TD: NLRP3 inflammasome in cancer and metabolic diseases. Nat Immunol 22: 550-559, 2021.
14. Hutton HL, Ooi JD, Holdsworth SR and Kitching AR: The NLRP3 inflammasome in kidney disease and autoimmunity. Nephrology (Carlton) 21: 736-744, 2016.
15. Wu M, Han W, Song S, Du Y, Liu C, Chen N, Wu H, Shi Y and Duan H: NLRP3 deficiency ameliorates renal inflammation and fibrosis in diabetic mice. Mol Cell Endocrinol 478: 115-125, 2018.
16. Kim Y, Lim JH, Kim MY, Kim EN, Yoon HE, Shin SJ, Choi BS, Kim YS, Chang YS and Park CW: The adiponectin receptor agonist adiporon ameliorates diabetic nephropathy in a model of type 2 diabetes. J Am Soc Nephrol 29: 1108-1127, 2018.
17. Dietrich A and Gudermann T: TRPC6. Handb Exp Pharmacol: 125-141, 2007 doi: 10.1007/978-3-540-34891-7_7.
18. Kong L, Sun R, Zhou H, Huang D, Xing W, Wu B, Li H, Hu W, Song S and Xu Y: Trpc6 knockout improves behavioral dysfunction and reduces Aβ production by inhibiting CN-NFAT1 signaling in T2DM mice. Exp Neurol 363: 114350, 2023.
19. Staruschenko A, Spires D and Palygin O: Role of TRPC6 in progression of diabetic kidney disease. Curr Hypertens Rep 21: 48, 2019.
20. Eder P: Cardiac remodeling and disease: SOCE and TRPC signaling in cardiac pathology. Adv Exp Med Biol 993: 505-521, 2017.
21. Ma R, Chaudhari S and Li W: Canonical transient receptor potential 6 channel: A new target of reactive oxygen species in renal physiology and pathology. Antioxid Redox Signal 25: 732-748, 2016.
22. Lin BL, Matera D, Doerner JF, Zheng N, Del Camino D, Mishra S, Bian H, Zeveleva S, Zhen X, Blair NT, *et al*: In vivo selective inhibition of TRPC6 by antagonist BI 749327 ameliorates fibrosis and dysfunction in cardiac and renal disease. Proc Natl Acad Sci USA 116: 10156-10161, 2019.
23. Nie B, Liu C, Bai X, Chen X, Wu S, Zhang S, Huang Z, Xie M, Xu T, Xin W, *et al*: AKAP150 involved in paclitaxel-induced neuropathic pain via inhibiting CN/NFAT2 pathway and downregulating IL-4. Brain Behav Immun 68: 158-168, 2018.
24. Rusnak F and Mertz P: Calcineurin: Form and function. Physiol Rev 80: 1483-1521, 2000.
25. Rao A, Luo C and Hogan PG: Transcription factors of the NFAT family: Regulation and function. Annu Rev Immunol 15: 707-747, 1997.
26. Mognol GP, Carneiro FR, Robbs BK, Faget DV and Viola JP: Cell cycle and apoptosis regulation by NFAT transcription factors: New roles for an old player. Cell Death Dis 7: e2199, 2016.
27. Ling H, Zhu Z, Yang J, He J, Yang S, Wu D, Feng S and Liao D: Dihydromyricetin improves type 2 diabetes-induced cognitive impairment via suppressing oxidative stress and enhancing brain-derived neurotrophic factor-mediated neuroprotection in mice. Acta Biochim Biophys Sin (Shanghai) 50: 298-306, 2018.
28. Wick MR: The hematoxylin and eosin stain in anatomic pathology-An often-neglected focus of quality assurance in the laboratory. Semin Diagn Pathol 36: 303-311, 2019.
29. Yang L, Guo J, Yu N, Song H, Niu J and Gu Y: Tocilizumab mimotope alleviates kidney injury and fibrosis by inhibiting IL-6 signaling and ferroptosis in UUO model. Life Sci 261: 118487, 2020.
30. Lefkowitch JH: Special stains in diagnostic liver pathology. Semin Diagn Pathol 23: 190-198, 2006.
31. Qiao S, Liu R, Lv C, Miao Y, Yue M, Tao Y, Wei Z, Xia Y and Dai Y: Bergenin impedes the generation of extracellular matrix in glomerular mesangial cells and ameliorates diabetic nephropathy in mice by inhibiting oxidative stress via the mTOR/β-TrcP/Nrf2 pathway. Free Radic Biol Med 145: 118-135, 2019.
32. Han WK, Bailly V, Abichandani R, Thadhani R and Bonventre JV: Kidney Injury Molecule-1 (KIM-1): A novel biomarker for human renal proximal tubule injury. Kidney Int 62: 237-244, 2002.
33. Glastras SJ, Chen H, Teh R, McGrath RT, Chen J, Pollock CA, Wong MG and Saad S: Mouse models of diabetes, obesity and related kidney disease. PLoS One 11: e0162131, 2016.
34. Jha JC, Banal C, Chow BS, Cooper ME and Jandeleit-Dahm K: Diabetes and kidney disease: Role of oxidative stress. Antioxid Redox Signal 25: 657-684, 2016.
35. Gong W, Luo C, Peng F, Xiao J, Zeng Y, Yin B, Chen X, Li S, He X, Liu Y, *et al*: Brahma-related gene-1 promotes tubular senescence and renal fibrosis through Wnt/β-catenin/autophagy axis. Clin Sci (Lond) 135: 1873-1895, 2021.

36. Yan Q, Sui W, Xie S, Chen H, Xie S, Zou G, Guo J and Zou H: Expression and role of integrin-linked kinase and collagen IV in human renal allografts with interstitial fibrosis and tubular atrophy. Transpl Immunol 23: 1-5, 2010.
37. Kharroubi AT and Darwish HM: Diabetes mellitus: The epidemic of the century. World J Diabetes 6: 850-867, 2015.
38. Chen XC, Li ZH, Yang C, Tang JX, Lan HY and Liu HF: Lysosome depletion-triggered autophagy impairment in progressive kidney injury. Kidney Dis (Basel) 7: 254-267, 2021.
39. Duan JY, Lin X, Xu F, Shan SK, Guo B, Li FX, Wang Y, Zheng MH, Xu QS, Lei LM, *et al*: Ferroptosis and its potential role in metabolic diseases: A curse or revitalization? Front Cell Dev Biol 9: 701788, 2021.
40. Al Mamun A, Ara Mimi A, Wu Y, Zaeem M, Abdul Aziz M, Aktar Suchi S, Alyafeai E, Munir F and Xiao J: Pyroptosis in diabetic nephropathy. Clin Chim Acta 523: 131-143, 2021.
41. Sifuentes-Franco S, Padilla-Tejeda DE, Carrillo-Ibarra S and Miranda-Díaz AG: Oxidative stress, apoptosis, and mitochondrial function in diabetic nephropathy. Int J Endocrinol 2018: 1875870, 2018.
42. Samsu N: Diabetic Nephropathy: Challenges in pathogenesis, diagnosis, and treatment. Biomed Res Int 2021: 1497449, 2021.
43. Luo Y, Lu Z, Waaga-Gasser AM, Yang H, Liu J, Wu J, Lu J, Liu X and Zhang L: Modulation of calcium homeostasis may be associated with susceptibility to renal cell carcinoma in diabetic nephropathy rats. Cancer Manag Res 12: 9679-9689, 2020.
44. Wang Q, Tian X, Wang Y, Wang Y, Li J, Zhao T and Li P: Role of transient receptor potential canonical channel 6 (TRPC6) in diabetic kidney disease by regulating podocyte actin cytoskeleton rearrangement. J Diabetes Res 2020: 6897390, 2020.
45. Yu J, Li C, Ma L, Zhai B, Xu A and Shao D: Transient receptor potential canonical 6 knockdown ameliorated diabetic kidney disease by inhibiting nuclear factor of activated T cells 2 expression in glomerular mesangial cells. Ren Fail 44: 1780-1790, 2022.
46. Zimmet P, Shi Z, El-Osta A and Ji L: Epidemic T2DM, early development and epigenetics: Implications of the Chinese Famine. Nat Rev Endocrinol 14: 738-746, 2018.
47. Vaidya VS, Ozer JS, Dieterle F, Collings FB, Ramirez V, Troth S, Muniappa N, Thudium D, Gerhold D, Holder DJ, *et al*: Kidney injury molecule-1 outperforms traditional biomarkers of kidney injury in preclinical biomarker qualification studies. Nat Biotechnol 28: 478-485, 2010.
48. Adeva-Andany MM, Adeva-Contreras L, Fernández-Fernández C, Carneiro-Freire N and Domínguez-Montero A: Histological Manifestations of diabetic kidney disease and its relationship with insulin resistance. Curr Diabetes Rev 19: e280322202705, 2023.
49. Lee BY, Han JA, Im JS, Morrone A, Johung K, Goodwin EC, Kleijer WJ, DiMaio D and Hwang ES: Senescence-associated beta-galactosidase is lysosomal beta-galactosidase. Aging Cell 5: 187-195, 2006.
50. Bellary S, Kyrou I, Brown JE and Bailey CJ: Type 2 diabetes mellitus in older adults: Clinical considerations and management. Nat Rev Endocrinol 17: 534-548, 2021.
51. Bülow RD and Boor P: Extracellular matrix in kidney fibrosis: More than just a scaffold. J Histochem Cytochem 67: 643-661, 2019.
52. Yuan Q, Tan RJ and Liu Y: Myofibroblast in kidney fibrosis: Origin, activation, and regulation. Adv Exp Med Biol 1165: 253-283, 2019.
53. Chen PS, Li YP and Ni HF: Morphology and evaluation of renal fibrosis. Adv Exp Med Biol 1165: 17-36, 2019.
54. Song MK, Lee JH, Ryoo IG, Lee SH, Ku SK and Kwak MK: Bardoxolone ameliorates TGF-β1-associated renal fibrosis through Nrf2/Smad7 elevation. Free Radic Biol Med 138: 33-42, 2019.
55. Fukasawa H, Yamamoto T, Suzuki H, Togawa A, Ohashi N, Fujigaki Y, Uchida C, Aoki M, Hosono M, Kitagawa M and Hishida A: Treatment with anti-TGF-beta antibody ameliorates chronic progressive nephritis by inhibiting Smad/TGF-beta signaling. Kidney Int 65: 63-74, 2004.
56. Ka SM, Huang XR, Lan HY, Tsai PY, Yang SM, Shui HA and Chen A: Smad7 gene therapy ameliorates an autoimmune crescentic glomerulonephritis in mice. J Am Soc Nephrol 18: 1777-1788, 2007.
57. Ka SM, Yeh YC, Huang XR, Chao TK, Hung YJ, Yu CP, Lin TJ, Wu CC, Lan HY and Chen A: Kidney-targeting Smad7 gene transfer inhibits renal TGF-β/MAD homologue (SMAD) and nuclear factor κB (NF-κB) signalling pathways, and improves diabetic nephropathy in mice. Diabetologia 55: 509-519, 2012.
58. Szabó C: Nitric oxide, intracellular calcium overload, and cytotoxicity. Shock 6: 25-26, 1996.
59. Han Y, Su Y, Han M, Liu Y, Shi Q, Li X, Wang P, Li W and Li W: Ginsenoside Rg1 attenuates glomerular fibrosis by inhibiting CD36/TRPC6/NFAT2 signaling in type 2 diabetes mellitus mice. J Ethnopharmacol 302: 115923, 2023.
60. Seo K, Rainer PP, Shalkey Hahn V, Lee DI, Jo SH, Andersen A, Liu T, Xu X, Willette RN, Lepore JJ, *et al*: Combined TRPC3 and TRPC6 blockade by selective small-molecule or genetic deletion inhibits pathological cardiac hypertrophy. Proc Natl Acad Sci USA 111: 1551-1556, 2014.
61. Reiser J, Polu KR, Möller CC, Kenlan P, Altintas MM, Wei C, Faul C, Herbert S, Villegas I, Avila-Casado C, *et al*: TRPC6 is a glomerular slit diaphragm-associated channel required for normal renal function. Nat Genet 37: 739-744, 2005.
62. Hofmann T, Obukhov AG, Schaefer M, Harteneck C, Gudermann T and Schultz G: Direct activation of human TRPC6 and TRPC3 channels by diacylglycerol. Nature 397: 259-263, 1999.
63. Kobayashi M, Mutharasan RK, Feng J, Roberts MF and Lomasney JW: Identification of hydrophobic interactions between proteins and lipids: Free fatty acids activate phospholipase C delta1 via allosterism. Biochemistry 43: 7522-7533, 2004.
64. Makarewich CA, Zhang H, Davis J, Correll RN, Trappanese DM, Hoffman NE, Troupes CD, Berretta RM, Kubo H, Madesh M, *et al*: Transient receptor potential channels contribute to pathological structural and functional remodeling after myocardial infarction. Circ Res 115: 567-580, 2014.
65. Koitabashi N, Aiba T, Hesketh GG, Rowell J, Zhang M, Takimoto E, Tomaselli GF and Kass DA: Cyclic GMP/PKG-dependent inhibition of TRPC6 channel activity and expression negatively regulates cardiomyocyte NFAT activation Novel mechanism of cardiac stress modulation by PDE5 inhibition. J Mol Cell Cardiol 48: 713-724, 2010.
66. Chung HS, Kim GE, Holewinski RJ, Venkatraman V, Zhu G, Bedja D, Kass DA and Van Eyk JE: Transient receptor potential channel 6 regulates abnormal cardiac S-nitrosylation in Duchenne muscular dystrophy. Proc Natl Acad Sci USA 114: E10763-E10771, 2017.
67. Wang L, Jirka G, Rosenberg PB, Buckley AF, Gomez JA, Fields TA, Winn MP and Spurney RF: Gq signaling causes glomerular injury by activating TRPC6. J Clin Invest 125: 1913-1926, 2015.
68. Su Y, Chen Q, Ju Y, Li W and Li W: Palmitate induces human glomerular mesangial cells fibrosis through CD36-mediated transient receptor potential canonical channel 6/nuclear factor of activated T cell 2 activation. Biochim Biophys Acta Mol Cell Biol Lipids 1865: 158793, 2020.
69. Bian Y, Shi C, Song S, Mu L, Wu M, Qiu D, Dong J, Zhang W, Yuan C, Wang D, *et al*: Sestrin2 attenuates renal damage by regulating Hippo pathway in diabetic nephropathy. Cell Tissue Res 390: 93-112, 2022.
70. Mena MP, Papiewska-Pajak I, Przygodzka P, Kozaczuk A, Boncela J and Cierniewski CS: NFAT2 regulates COX-2 expression and modulates the integrin repertoire in endothelial cells at the crossroads of angiogenesis and inflammation. Exp Cell Res 324: 124-136, 2014.
71. Zhang D, Ji P, Sun R, Zhou H, Huang L, Kong L, Li W and Li W: Ginsenoside Rg1 attenuates LPS-induced chronic renal injury by inhibiting NOX4-NLRP3 signaling in mice. Biomed Pharmacother 150: 112936, 2022.
72. Shahzad K, Fatima S, Khawaja H, Elwakiel A, Gadi I, Ambreen S, Zimmermann S, Mertens PR, Biemann R and Isermann B: Podocyte-specific Nlrp3 inflammasome activation promotes diabetic kidney disease. Kidney Int 102: 766-779, 2022.
73. Li S, Zheng L, Zhang J, Liu X and Wu Z: Inhibition of ferroptosis by up-regulating Nrf2 delayed the progression of diabetic nephropathy. Free Radic Biol Med 162: 435-449, 2021.